# Design and Analysis of Diesel Engine Exhaust Manifolds for Genset Engine

**Mr. Eshwar S. Korade[1] Prof. B. M. Randhavan[2]**
[1,2]Department of Mechanical Engineering
[1,2]Sahyadri Valley College of Engineering, India

*Abstract*— Exhaust manifold is an important component in an exhaust system of engine. It connects to each exhaust port on the engine's cylinder head, and it funnels the hot exhaust down into one simple exhaust pipe. With the help of the exhaust manifold gaskets, it also prevents the toxic exhaust fumes from sneaking into the vehicle and harming the occupants. This paper is related to design and finite element analysis of exhaust manifold of 4 cylinder diesel engine. Engine capacity is 5678cc. The finite element analysis in ANSYS software by using materials based on their composition viz. FG220MoCr and SG500/7. In FEA we find out the thermal as well as static structural properties material. Finally the results are validated through experimentation on tensile strength, Izod-Charpy impact testing, and Metallurgical Microscope.

***Keywords:*** Exhaust Manifold, Finite Element Analysis, Modal Analysis

## I. Introduction

In Exhaust plays a crucial role in the performance of any internal combustion engine. The exhaust system begins with manifolds on the engine and ends with the tail pipe. Basically, it includes an exhaust manifold, heat riser, exhaust pipe, catalytic converter, muffler, resonator (optional), and tail pipe. Following is a closer look at each component.

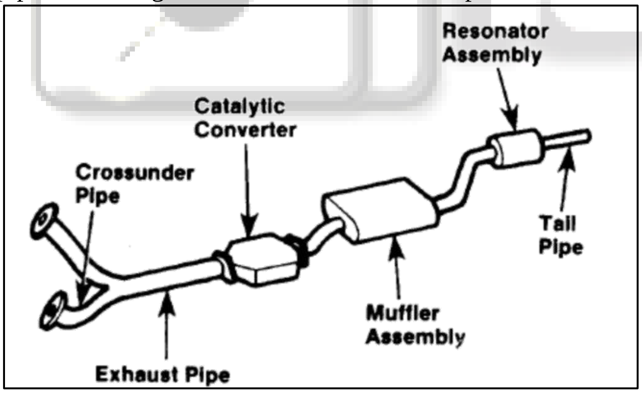


Fig. 1.1" Typical Exhaust System

The exhaust manifold collects the burned gases as they are expelled from the engine cylinders and directs them to the exhaust pipe. The manifold is designed to give minimum back pressure and turbulence. Exhaust system should be designed keeping in mind the allowable back pressure will be half of the maximum permissible. Restriction of backpressure is generally due to pipe size, silencer, and system configuration. Catalyst products utilize dry, water cooled and air shielded water cooled (ASWC) manifold designs, based on application and design requirements. Dry manifolds are the preferred manifold design. They are cost effective and by providing the maximum possible exhaust energy to the turbocharger, they offer the highest overall efficiency. Dry manifolds, however, also radiate the most heat and reach the highest surface temperatures.

In this paper we create a three dimensional model of Exhaust manifold in CATIA V5R modeling software. Static structural analysis done in ANSYS 14.5 (FEA) software by using two different materials based on their composition. Exhaust manifolds are manufactured using cast iron. So the exhaust manifold material FG220MoCr is replaced by material such as SG500/7.

## II. Literature Review

The fuel manifold is an import accessory through which the fuel enters in combustor, after measuring in fuel control system. The component test results of fuel manifolds show that , when the starting fuel supply is given and the primary fuel manifold relative unfold pressure is at constant, the adjustment of the secondary fuel manifold turn-on pressure has effects on fuel flow through the secondary fuel manifold and the time of fuel into the combustion chamber. The verification test of the secondary fuel manifold unfold pressure influence on engine starting performance has been conducted, showing that the unfold pressure variation of the secondary fuel manifold has great influence on the engine start performance. The test research results have important guidance and reference meaning for confirming the secondary fuel manifold unfolds pressure. [1]

The computational challenges encountered in turbocharger turbine and exhaust manifold flow analysis. The core computational method is the Space–Time Variational Multiscale (ST-VMS) method, and the other key methods are the ST ISO geometric Analysis (ST-IGA), ST Slip Interface (ST-SI) method, ST/NURBS Mesh Update Method (STNMUM), and a general-purpose NURBS mesh generation method for complex geometries. The ST framework, in a general context, provides higher-order accuracy. The VMS feature of the ST-VMS addresses the computational challenges associated with the multiscale nature of the unsteady flow in the manifold and turbine, and the moving-mesh feature of the ST framework enables high-resolution computation near the rotor surface. The ST-SI enables moving mesh computation of the spinning rotor. The mesh covering the rotor spins with it, and the SI between the spinning mesh and the rest of the mesh accurately connects the two sides of the solution. The ST-IGA enables more accurate representation of the turbine and manifold geometries and increased accuracy in the flow solution. The STNMUM enables exact representation of the mesh rotation. The general-purpose NURBS mesh generation method makes it easier to deal with the complex geometries we have here. An SI also provides mesh generation flexibility in a general context by accurately connecting the two sides of the solution computed over no matching meshes. That is enabling us to use no matching NURBS meshes here. Stabilization parameters and element length definitions play a significant role in the ST-VMS and ST-SI. For the ST-VMS, we use the stabilization parameters introduced recently, and for the ST-SI, the element length definition we are introducing here. The model we actually compute with includes the exhaust gas purifier, which makes the turbine outflow conditions more realistic. We compute the flow for a full intake/exhaust cycle, which is much longer than the turbine rotation cycle because of high rotation speeds, and the long duration required is an additional computational challenge. The computation demonstrates that the methods we use here are very effective in this class of challenging flow analyses. [2]

Some mechanical components are subjected to thermo-mechanical fatigue, which occurs when both thermal and mechanical loads vary with time. Due to the complexity of the components geometry, stresses and strains field becomes multiaxial, worsening the fatigue resistance. In this paper several damage models are applied and compared on a case study, an automotive exhaust manifold simulacrum replying the material and the geometrical features of the commercial component. A complete thermo-structural FE analysis has been run and results have been post-processed by means of a numerical code implementing several multiaxial damage models available in literature and based both on a critical plane approach (Kandil-Brown-Miller, Fatemi-Socie) and strain-based models (Von Mises, ASME Code and Sonsino-Grubisic). The model calibration has been carried out by means of literature experimental data referred to commercial exhaust manifolds of similar geometry and material. [3]

Out-of-phase thermo mechanical fatigue (OP-TMF) tests between 600qC and 950qC have been conducted for three cast austenitic alloys with different metal-carbide (MC) morphologies: dense skeleton, sparse skeleton and blocky carbides. The alloy with dense skeleton-like MC exhibited longer TMF life than the other two, even though their chemical composition and casting process were similar. Fractographic analysis indicated that the fatigue cracks initiated from the specimen surface for all the alloys in this study. The morphology of Nb (C, N) has an obvious effect on inelastic deformation. Alloys with skeleton-like Nb(C, N) precipitates have better ductility as compared to alloys with isolated blocky precipitates. Dense skeleton-like Nb(C, N) is found to delay OP-TMF crack initiation and propagation, resulting in longer TMF lives. [4]

Due to the more stringent and upcoming laws in terms of environment protection field, the required temperatures in combustion chamber need to be higher in order to reduce particles emissions. This target is reached by engine downsizing (see FIAT and Ford) together with the application of turbochargers, but the new altered conditions lead to a design of exhaust gas manifold that has to take into account an improvement in terms of temperature up to 1050°C. Above all, materials characterization has to be carried out in order to represent, as close as possible, real operative conditions. Usually, materials for exhaust gas manifold are characterized from HCF, LCF and TMF point of view by testing on cylindrical specimens, but this way it's not possible to detect the effect given by rolling process. In these last years CRF has designed and developed a particular kind of anti-buckling in order to allow LCF and TMF characterization on flat specimen at high temperatures with fully reversed strain cycle. This paper will show the results of LCF characterization carried out on flat specimen (th=1.5 [mm]) in strain ratio condition $R\varepsilon=-1$ at temperatures of 600[°C] and 800[°C]. Furthermore, results of several TMF tests will be showed. [5]

A naturally aspirated, direct injection diesel engine investigating of combustion and emission characteristics of $CH_4$-$CO_2$ and $CH_4$-$CO_2$-$H_2$ mixtures has studied. These aspirated gas mixtures were pilot-ignited by diesel fuel, while the engine load was varied between 0 and 7 bar IMEP by only adjusting the flow rate of the aspirated mixtures. The in-cylinder gas composition was also investigated when combusting $CH_4$-$CO_2$ and $CH_4$-$CO_2$-$H_2$ mixtures at different engine loads, with in cylinder samples collected using two different sampling arrangements. The results showed a longer ignition delay period and lower peak heat release rates when the proportion of $CO_2$ was increased in the aspirated mixture. Exhaust $CO_2$ emissions were observed to be higher for $60CH_4{:}40CO_2$ mixture, but lower for the $80CH_4{:}20CO_2$ mixture as compared to diesel fuel only combustion at all engine loads. Both exhaust and in-cylinder $NO_x$ levels were observed to decrease when the proportion of $CO_2$ was increased; $NO_x$ levels increased when the proportion of $H_2$ was increased in the aspirated mixture. In-cylinder $NO_x$ levels were observed to be higher in the region between the sprays as compared to within the spray core, attributable to higher gas temperatures reached, post ignition, in that region. [6]

The current scenario of high growth rate of automobile usage, the automobile industry is forced to adopt the government emission norms to keep the environment green. Latest technologies have been developed in the automotive exhaust system to acknowledge the emission norms. Diesel oxidation catalyst and Muffler both are playing major roles in reducing emission and noise level as well. Diesel oxidation catalyst reduces CO and unburned HC emissions. Muffler reduces noise level of exhaust gases. Nowadays automobile industry is using CFD software extensively to analyze the flow properties inside the diesel oxidation catalyst and Muffler. Flow analysis helps to optimize the geometric design of Diesel oxidation catalyst to oxidize the CO and unburned HC of exhaust gases. In this present work we studied pressure drop and uniformity index of an existing exhaust system which consists of close couple catalytic convertor, under body catalytic convertor and muffler. Exhaust system has been modeled by using CATIA V5 which is advanced CAD software. The substrate has been modeled as porous medium for analysis purpose. These models have been imported in CFD tool for analysis. After importing the CAD data inside the CFD software, with proper boundary conditions, the CFD analysis has been carried out. Based on the study, individual system contributions to the total pressure drop and flow uniformity have been analyzed and improvement areas of the existing system for better flow uniformity have been suggested. [7]

Intake manifold water injection (IMWI) is an effective way to control combustion temperature and $NO_x$ emission for diesel engines. The various effects of IMWI on diesel combustion and emissions reflect on the dilution effect, thermal effect and chemical effect. However, researchers have paid little attention to investigate the three effects. In this study, the dilution, thermal and chemical effects of IMWI on the combustion and emissions characteristics of a four-stroke, direct injection as well as turbocharged diesel engine are investigated by CFD simulation. The results indicate that IMWI reduces the in-cylinder mean pressure and temperature, and the ignition delay becomes longer. IMWI leads to a remarkable decrease of NOx and Soot emissions. Comparing to the thermal effect and chemical effect, the dilution effect of IMWI on engine combustion and emissions plays a dominant role. [8]

## III. PROBLEM STATEMENT

As power and torque increases the temperature of exhaust gases increases, this high temp fails the exhaust manifold with current material FG220MoCr. Hence we are selecting a new material without compromising functionality of Exhaust Manifold. Also thermal stresses should be kept as minimum.

## IV. OBJECTIVES

The aim at the end of this project is to predict the problem occurred in internal combustion engine exhaust manifold is high temperature and hence failure of exhaust manifold takes place. In achieving this aim, project objectives are set as below:

– To design of an exhaust manifold for the new proposed material.
– To analyze of the designed exhaust manifold using ANSYS 14.5.
– To Study the parameter like von misses stress, von misses strain and displacements were obtained from computational analysis software.
– To analyze an exhaust manifold without compromising properties of material.

## V. METHODOLOGY

– Theoretical calculation of four cylinder diesel engine exhaust manifold.
– Solid model of four cylinder exhaust manifolds.
– Meshing of 3-D entity of exhaust manifold.
– Finite element analysis in ANSYS14.5
– Computational results.
– Experimentation on material.
– Compare theoretical, FEA and experimental result.
– Engine Specifications

| Sr. No. | Type | 4 Cylinder Diesel Engine (Value) |
|---|---|---|
| 1 | Capacity of engine | 5678cc |
| 2 | Number of cylinder | 4 |
| 3 | Bore × Stroke | 97mm × 128 mm |
| 4 | Type of Injection | DI |
| 5 | Prime power | 115 kw @ 1500 rpm. |
| 6 | Maximum Torque | 732 Nm @ 1500 rpm. |
| 7 | Compression Ratio | 17.5:1 |

Table 6.1: Specification of 697 Genet engine

## VI. ANALYSIS BY ANSYS SOFTWARE

Exhaust plays a crucial role in the performance of any internal combustion engine. Its un reasonable limitation of flow can result in extra fuel consumption, increased exhaust temperature and smoke. It also results in decrement of exhaust valve life. It is mandatory to maintain a specific limit of back pressure in exhaust system else it will increase emissions. Exhaust system should be designed keeping in mind the allowable back pressure will be half of the maximum permissible. Restriction of backpressure is generally due to pipe size, silencer, and system configuration. Here, exhaust coming out of combustion chamber enters a box passing through separate compartment in it. It was assumed that high velocity smoke particle on entering in the box chamber gets reflected in several direction such that it will interfere with particles coming out of each pipe. Geometry of box was designed such that fraction of particle of each pipe interfere with the other one, resulting in extra sound reduction.

The designed 3D models of exhaust manifolds in CATIA software as shown in below figure:

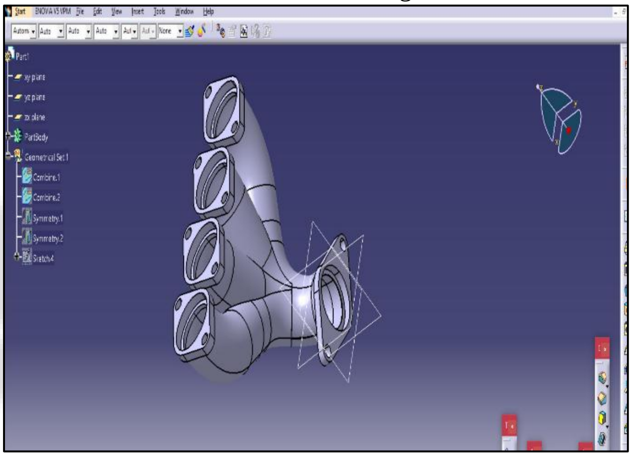

Fig. 7.1: 3d Model of Exhaust manifold in CATIA Software

### A. *Temperature Assumptions*

Temperature is an independent property for modulus of elasticity & thermal expansion coefficients are taken for the analysis as temperature dependent.

For Exhaust Manifold ~750°C
Exhaust Manifold Clamps~650°C
Turbocharger, EGR flange & surrounding region~650°C
Head region surrounding manifold face~200°C
Bolt thread region in side head~200°C
Bolt region at manifold contact~650°C

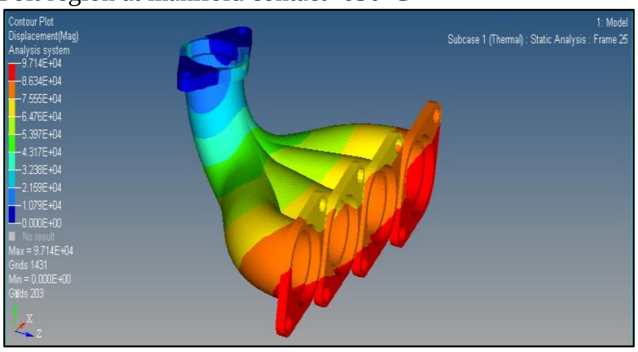


Fig. 7.2: Displacements – Thermal Analysis of Exhaust Manifolds

### *B. Analysis of Exhaust Manifolds*

Analysis of Exhaust Manifolds-
Material: FG220MoCr
Ultimate Compressive Strength = 220 MPa -550MPa
Poisson ratio: 0.3
Density: - 7500 kg/m3
Young's Modules: 200 GPa.

| Sample Identification | Chemical Composition % | | | | | | | | |
|---|---|---|---|---|---|---|---|---|---|
| | C | Si | Mn | S | P | Cr | Ni | Mo | Fe |
| FG220MoCr | 3.39 | 2.4 | 0.63 | 0.08 | 0.088 | -- | -- | -- | Bal |

Table 7.1: Chemical Composition of FG 220MoCr Material

B) Material: - SG500/7
Ultimate Compressive Strength = 320 MPa -416MPa
Poisson ratio: 0.29
Density: - 7100 kg/m3
Young's Modules: - 205MPa.

| Sample Identification | Chemical Composition % | | | | | | | | |
|---|---|---|---|---|---|---|---|---|---|
| | C | Si | Mn | S | P | Cr | Ni | Mo | Fe |
| SG500/7 | 3.36 | 2.8 | 0.13 | 0.15 | 0.005 | -- | -- | -- | Bal |

Table 7.2: Chemical Composition of SG 500/7 Material

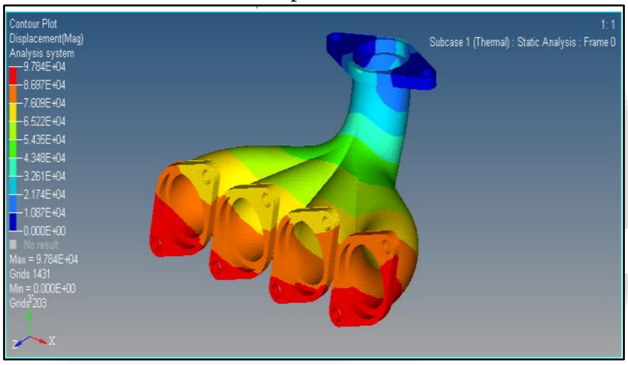


Fig. 7.3: Dsplacements – Thermal Analysis of Exhaust Manifolds

## VII. EXPERIMENTATION WORK

### *A. Impact Test*

Notched-bar impact test of metals provides information on failure mode under high velocity loading conditions leading sudden fracture where a sharp stress raiser (notch) is present. The energy absorbed at fracture is generally related to the area under the stress-strain curve which is termed as toughness in some references. Brittle materials have a small area under the stress-strain curve (due to its limited toughness) and as a result, little energy is absorbed during impact failure. As plastic deformation capability of the materials (ductility) increases, the area under the curve also increases and absorbed energy and respectively toughness increase. The fracture surfaces for low energy impact failures, indicating brittle behaviour, are relatively smooth and have crystalline appearance in the metals. On the contrary, those for high energy fractures have regions of shear where the fracture surface is inclined about 45° to the tensile stress, and have rougher and more highly deformed appearance, called fibrous fracture. Although two standardized tests, the Charpy and Izod, were designed and used extensively to measure the impact energy, Charpy V-notched impact tests are more common in practice. The apparatus for performing impact tests is illustrated schematically in Figure 6.3. The load is applied as an impact blow from a weighted pendulum hammer that is released from a position at a fixed height h. The specimen is positioned at the base and with the release of pendulum, which has a knife edge, strikes and fractures the specimen at the notch. The pendulum continues its swing, rising a maximum height h' which should be lower than naturally. The energy absorbed at fracture E can be obtained by simply calculating the difference in potential energy of the pendulum before and after the test such as

$$E = m \times g \times (h - h^{'})$$

Where,

$m =$ The mass of pendulum, $g =$ Acceleration of gravity.

The geometry of 100 mm long, standard Charpy test specimen is given in Figure 6.2 If the dimensions of specimens are maintained as indicated in standards, notched-bar impact test results are affected by the lattice type of materials, testing temperature, thermo-mechanical history, chemical composition of materials and degree of strain hardening. Body cantered cubic (bcc) metals, particularly steels, often exhibit a decrease in impact energy as the temperature is lowered.

#### *1) Specimen Preparation for Impact Test*

a) Charpy Impact Test Specimen

In this test a specimen is used as a simply supported beam. A single blow of hammer is given at the mid span of the specimen. The low should be sufficient to bend or break the specimen of square cross section 6.25 mm×10 mm× and 50 mm in length with 45° V notch at the centre. The Striking energy should be $310 \pm 10$ joules. The Energy in the bending or breaking the specimen is taken as "Charpy impact Value" The Dimensions of the standard specimen are as given in following diagram.

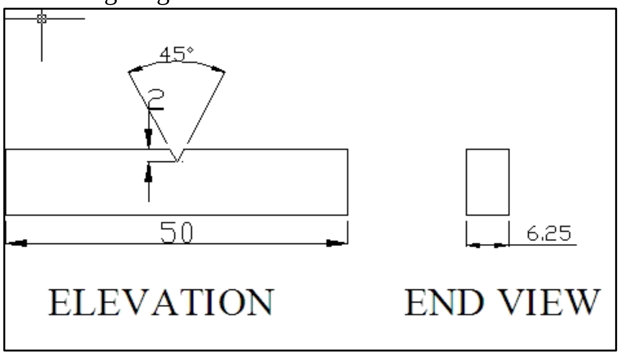


Fig. 8.1: Charpy Impact Test Specimen (As per ASTM)

b) Izod Impact Test Specimen:

In this test the metal specimen is used as a vertical cantilever, fixed at the bottom and free at the top. A single blow of hammer is given to the free end of the specimen. The blow should be sufficient to bend or break the specimen. The striking energy should be $165.8 \pm 3.4$ Joules. The energy spent in bending or breaking the specimen is taken as "Izod Impact Value" Standard square test specimen for Izod Impact test has a 45° V notch at the breaking Section. The Dimension of the standard specimen is given below.

 

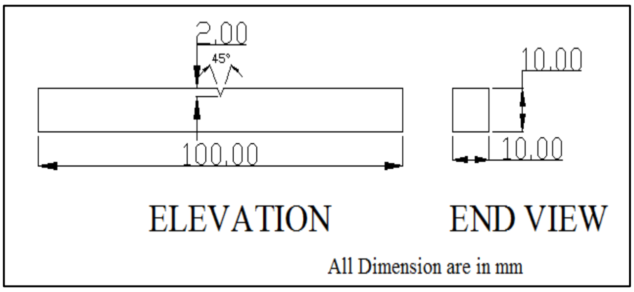


Fig. 8.2: Izod Impact Test Specimen (As per ASTM)

*2) Process Setup for Impact Test*

Materials sometimes display brittleness which precludes their use in a given design. Brittleness is characterized by fracturing with low energy under impact. The fracture energy is proportional to the area under the tensile stress-strain curve and is called the toughness. Tough steel is generally ductile and requires 100 ft-lbs of energy to cause failure. Brittle steel does not deform very much during failure and requires less than 15 ft- lbs energy to cause failure. Characterizing the toughness of a material is done in several ways. The most common method is the notched-bar impact test for which two types of specimens prevail, Charpy and Izod. By subjecting a specimen to an impact load, it will fail if the load exceeds the breaking strength of the material. By using a swinging pendulum to impart the load, the energy required to fracture the specimen can be calculated by observing the height the pendulum swings after fracture, as shown in below Figure.

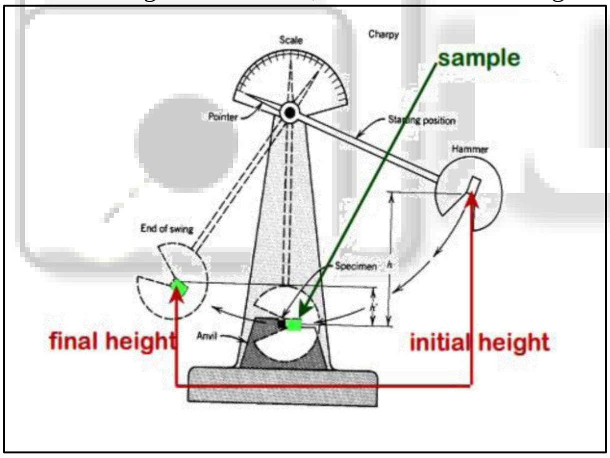


Fig. 8.3: Schematic Diagram of Experimental Setup for Impact Test

Fig. 8.4: Process Setup for Impact Test

*3) Impact Test Procedure*

For each test run the following procedures have to be followed:

1) Insure that the pointer of the dial counter has zero rest.
2) Raise the pendulum hammer to the required height of the impact tester. Release the hammer allowing a free Swing when there is no specimen and record the initial energy.
3) Raise the pendulum to the same height as before and clam it. Adjust the energy pointer to initial position.
4) Fix the specimen as a vertical cantilever in anvil box. The notch shall face the striking hammer and shall be half inside and half above the top surface of the anvil.
5) Once the specimen is secured and the path of the pendulum swing is clear, release it by pushing forward firmly on the release-handle. The hammer strikes the specimen. The specimen bends or breaks. The hammer swings to and fro. Stop the hammer by applying breaks.
6) Observe the reading on the scale and record it as the final energy. Also observe and record the failure pattern of the specimen.
7) Repeat the procedure for the specimen of different selected material.

## VIII. EXPERIMENTAL TEST RESULT

### *A. Analysis Result:*

| Sr. No. | Material Identification | Maximum Von Misses (N/mm$^2$) | Displacements (mm) | Maximum Principal Stress (N/mm$^2$) | Minimum Principal Stress (N/mm$^2$) | Mass (Kg) |
|---|---|---|---|---|---|---|
| 1 | FG220MoCr | 0.587E+04 | 0.978E+05 | 0.1129E+09 | 0.1028E+09 | 4.667 |
| 2 | SG500/7 | 0.5534E+04 | 0.971E+05 | 0.9088E+09 | 0.8271E+05 | 4.285 |

### *B. Hardness Test Results*

| Sr. No. | Sample Material | Diameter of in indenter (Ø ) in mm | Test load (F) N | BHN |
|---|---|---|---|---|
| 1 | FG220MoCr | 5 | 100 | 182 |
| 2 | SG500/7 | 5 | 100 | 198 |

### *C. Metallurgical Test Result:*

All the samples of two materials are observed under microscope. These tests are conducted on Microphotograph with maximum magnification of 100x for FG220MoCr and SG 500/7. Results are shown as follows.

#### *1) Result of FG 220MoCr*

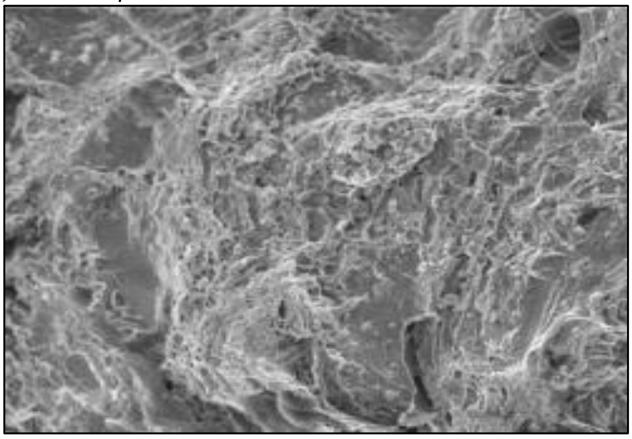

Fig. 8.1: Microstructure of FG220MoCr Material

a) Comments:

It Shows graphite flake in the ferritic matrix with dark band of pearlite of the cell boundaries. Over all dendritic pattern. Flake size is ASTM B TYPE size is about ASTM 3. Large casting defect (shrinkage pore, Figure No: - 7.1) was observed in the final fracture portion of this sample.

#### *2) Result of SG 500/7*

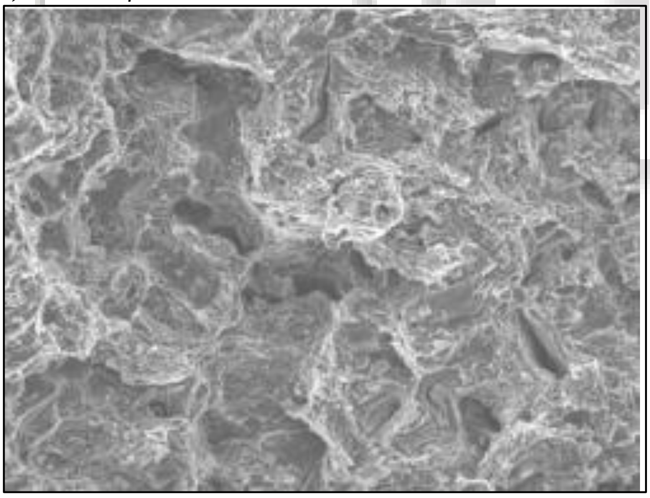

Fig. 8.2: Microstructure of SG500/7 Material

a) Comments:

It was in fact needed to combine the images taken by SEM, the fracture surface is relatively less flat as compared to FG220MoCr consistent with the observed lower fatigue life for this SG500/7 Perlites structure with grain boundary cementite is observed. It shows graphite flake with interdendric segregation. Flakes are mainly type D (Random Orientation). It some are the type E (Preferred Orientation) possibly due to inadequate inoculation.

## IX. CONCLUSION

### *A. Finite Element Analysis*

- The maximum displacements appear for new material is less than the original material.
- The stresses induced in new material also less than nearly 5% than original material.
- An experimental stress and FEA results gives close agreement, within 7% difference.

### *B. Experimental Test Analysis*

- Hardness of new material is high than the original material.
- From impact test we can replace new material to original material for better results of exhaust manifold.

## REFERENCES

[1] Jianbing Cain, Gaiqi Li, Jianhua Li, Yi Hu, "Study on effects of the secondary fuel manifold unfold pressure on engine starting performance", Propulsion and Power Research (2017), vol-6, issue-4, 253-258.

[2] Yuto Otoguroa, Kenji Takizawaa,_, Tayfun E. Tezduyar, Kenichiro Nagaokaa, Sen Mei, "Turbocharger turbine and exhaust manifold flow computation with the Space–Time Variational Multiscale Method and Isogeometric Analysis", An International Journal of Computers & Fluids (2018).

[3] Cristiana Delprete, Raffaella Sesana, Andrea Vercelli, "Multiaxial damage assessment and life estimation: application to an automotive exhaust manifold", Procedia Engineering 2 (2010) 725–734.

[4] Hailong Zhao, Carlos C. Engler-Pinto Jr. , Jacob Zinde , Larry Godlewski , Yinhui Zhang , Qiang Feng , Mei Lib , "The Effect of Metal-Carbide Morphology on the Thermomechanical Fatigue (TMF) Behavior of Cast Austenitic Alloys for Exhaust Manifolds", Procedia Engineering 133 ( 2015 ) 669 – 680.

[5] Xiaoping Chen, Xiaoli Yu, Rufu Hu, Jianfeng Li, "Statistical distribution of crankshaft fatigue: Experiment and modeling", Engineering Failure Analysis 42 (2014) 210–220.

[6] Midhat Talibi, Paul Hellier, Nicos Ladommatos, "Combustion and exhaust emission characteristics, and in-cylinder gas composition, of hydrogen enriched biogas mixtures in a diesel engine", Energy 124 (2017) 397-412.

[7] Om Ariara Guhan C Pa, Arthanareeswaren G a, Varadarajan K N, "CFD Study on Pressure Drop and Uniformity Index of Three Cylinder LCV Exhaust System", Procedia Engineering 127 (2015) 1211 – 1218.

[8] Xiaokang Ma, Fujun Zhang, Kai Han, Zhenxia Zhu, Yang yang Liu, "Effects of Intake Manifold Water Injection on Combustion and Emissions of Diesel Engine", Energy Procedia 61 ( 2014 ) 777 – 781.

 